Structural, Optical and Mechanical Property Analysis of Zinc Sulphate Admixtured L-arginine: A Novel Optoelectronic Material

P. Horsley Solomon, SRM Arts & Science College, Chennai, India, horsleysolomon@gmail.com

Dr. Johanan Christian Prasana, Madras Christian College, Chennai, India.

ABSTRACT - L-Arginine is an important amino acid due to their property of frequency conversion and electro optic modulation. In the present investigations, an attempt is made to grow single crystals of zinc sulphate admixtured L-arginine in different compositions by slow evaporation technique. Good quality single crystal with dimension 58 × 5 × 10 mm^3 is harvested after 60 days. The powder X-ray diffraction pattern of the crystal has been indexed. The optical absorption spectrum of the crystal presented good optical transparency in the entire visible region with ultra violet cut-off wavelength at 250 nm. The presence of different functional groups and connectivity of bonds are identified by Fourier Transform Infra Red spectral analysis (FT-IR) and Nuclear Magnetic Resonance (NMR) spectral analysis. The stability and thermal behaviour of the crystal is studied using Thermal Gravimetric Analysis (TGA). The crystal is subjected to Energy dispersive X-ray analysis (EDAX) measurements. The second harmonic generation (SHG) efficiency of zinc sulphate admixtured L-arginine crystal is found to have different behaviour response as compared to that of potassium di-hydrogen phosphate crystal.

Keywords: ***L-Arginine, Amino acid, zinc sulphate, Energy Dispersive X-ray Analysis, Fourier Transform Infra Red spectral analysis, Nuclear Magnetic Resonance spectral analysis***

I INTRODUCTION

Non linear optics is a fascinating research area over the past few decades, due to its multiple contributions in all fields of science & technology. The novel search for new nonlinear optical crystals was developed with improved optical properties for the utility of organic light emitting diode (OLED) applications. Most of the amino acids showed optical nonlinearity as they contain a proton donor carboxyl (-COOH) group and a proton acceptor amino group (NH_2) in the structural arrangements. Hence complexes of amino acids naturally exhibited nonlinearity with enhanced structural and physical properties towards innovative applications.

II. LITERATURE REVIEW

In the past few decades, there has been considerable interest in growth and characterization of nonlinear optical materials (NLO) due to their significant contributions in the multiple research areas such as frequency shifting, modulation, switching, logics and storage using optics. Experiments have been carried out for the exploration of nonlinear optical materials which find various applications in optoelectronics [1–7]. Optical second harmonic generation (SHG) uses the variances of amino acids and salts as they are highly reliable and tend to combine the advantages of organic amino acids with those of the inorganic acids/salts.

Crystalline semi-organic compounds of amino acids have recently fascinated considerable interest among researchers. The amino acid group materials have been mixed with inorganic salts to form admixtures or complexes in order to improve their mechanical, thermal and NLO properties [4-8]. The inability of organic compounds to grow a large crystal size for device fabrication, which has led to the discovery of a new class of crystals called semi organics to satisfy technological requirements [9, 10]. The most promising structural candidates among metal-organic compounds preferably zinc sulphate admixture amino acids have attracted researchers in recent years due to their various properties such as NLO response, magnetism, and luminescence. They are also used in photography and drug delivery due to the combination of organic and inorganic components.

In the semi-organic materials, the organic ligand is ionically bonded with the inorganic host, which promotes exceptional mechanical strength and chemical stability [11]. Because of this, semiorganic materials are promising for many other applications such as frequency conversion, light amplitude and phase modulation and phase conjugation [12].

 DOI : 10.18231/2454-9150.2018.1145

The metal–organic complexes offer higher environmental stability combined with greater diversity of tunable electronic properties by virtue of the coordinated metal centre [13]. Furthermore, organic ligands combined with inorganic salts thereby grow semi-organic crystals, which lead to more impressive applications such as second and third harmonic generations (SHG&THG), optical bistability, laser remote sensing, optical disc data storage, laser driven fusion, medical and spectroscopic image processing, colour displays and optical communication [14]. With this view, an attempt is made to grow new amino acid with inorganic salt based nonlinear optical crystals. This has resulted in the realization of crystals showing nonlinear optical properties appropriate for device applications.

In this present investigation the single crystal of pure zinc sulphate hexa hydrate and L-arginine doped zinc sulphate hexa hydrate has been grown by slow evaporation method. Zinc sulphate hexa hydrate (ZnSH) crystals are widely used for UV light filters and UV sensors [15-17]; however they possess moisture regaining property.

In the present examination a semi organic crystal of L-arginine Zinc sulfate (LAZnS) with various proportions has been developed effectively and the crystals subjected for different portrayals. This part manages the development of $LA_xZnS_{(1-x)}$ single crystals with various estimations of (x = 0, 0.2, 0.4, 0.6 and 0.8) utilizing moderate dissolvable dissipation procedure and the portrayal concentrates. For example, single crystal X-ray diffraction (XRD), powder XRD, Fourier transform infra red (FT-IR), optical ingestion, mechanical and dielectric properties have been studied with AC and DC conductivity. Kurtz and Perry SHG test have affirmed the NLO property of the developed precious stones.

III MATERIALS USED

Expository reagent (AR) review tests of L-arginine and Zinc sulfate were purchased from Merck India Ltd. Twofold refined water was utilized as the dissolvable for the development of $LA_xZnS_{(1-x)}$ single precious stones.

A. Preparation of semi organic crystals

$LA_xZnS_{(1-x)}$ was blended from L-arginine and Zinc sulfate, taken in the distinctive creations (0.2:0.8 , 0.4:0.6, 0.6:0.4 and 0.8:0.2) is broke down in twofold refined water. The arrancrystalent was mixed well and sifted utilizing fantastic channel papers of pore estimate under 1 mm. The separated arrancrystalent was kept for moderate dissipation at room temperature (30 °C). Modest precious stones were seen in the test vessels following 12 days of dissipation. A recrystalli-zation procedure was completed so as to dispense with debasements in the $LA_xZS_{(1-x)}$ precious stones.

1. Solubility

Solubility is one the most important physical parameter for the growth of good quality crystals at low temperature by slow evaporation method. The dissolvability of $LA_xZnS_{(1-x)}$ (x = 0.2,0.4,0.6,0.8) salts in twofold refined water was resolved for six distinct temperatures (25, 30, 35, 40, 45 and 50 °C) to arrive different semi organic crystals. The temperature subordinate solvency of $LA_xZnS_{(1-x)}$ precious stones are shown in Figure 1.

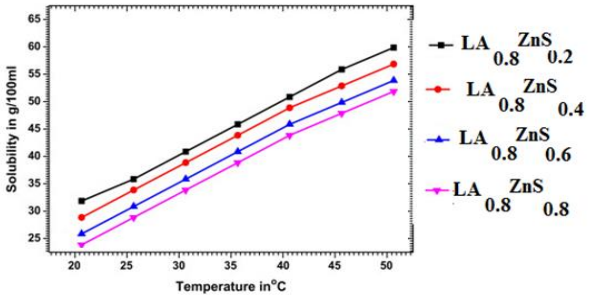

Figure 1: Solubility curve of $LA_xZnS_{(1-x)}$ single crystals

It is observed that the dissolvability of $LA_xZnS_{(1-x)}$ crystals increments with increment of temperature from 25 °C to 50 °C.

2. Growth of $LA_xZnS_{(1-x)}$ Single Crystals

As per the solubility information, the supersaturated arrancrystalent of $LA_xZnS_{(1-x)}$ was prepared. Single crystals of $LA_xZnS_{(1-x)}$ were developed by following slow evaporation method. The semitransparent, great quality precious stones were collected after 30-40 days. The obtained single precious stones of $LA_xZnS_{(1-x)}$ are shown in Figure 2.

Figure 2: Photograph of $LA_xZnS_{(1-x)}$ single crystals

B. Characterization

The single crystal X-beam information were collected and utilizing a programmed X beam diffractometer (MESSRS ENRAF NONIUS, The Netherlands) with MoK (λ= 0.717 Å) radiation. The naturally ground powder tests of LAZnS with different compositions of precious stones were subjected to powder X-beam diffraction (PXRD) examination, utilizing a X-beam powder diffractometer, PAN investigative with glimmer counter and monochromated Cu Kα (λ = 1.54056 Å) radiation. The FT-IR spectral analysis was performed in the range of 4000 – 400 cm^{-1} by BRUKER IFS 66V FT-IR Spectrometer. The optical assimilation range was recorded in the range of 190-800 nm utilizing VARIAN

 DOI : 10.18231/2454-9150.2018.1145

CARY 5E UV-Vis-NIR Spectrophotometer. The NLO effectiveness of $LA_xZnS_{(1-x)}$ crystals were analyzed by Kurtz and Perry powder method utilizing Q-exchanged Nd:YAG laser. The microhardness test was carried out by using Clemex CMT hardness framework. Static spaces were made at room temperature with a steady space time of 30 seconds. The space marks were made on the surfaces to differ the heap from 5 to 25 g. Dielectric steady, dielectric misfortune and the AC conductivity of the developed precious stones were estimated to a precision of ± 2% by LCR meter (Agilent 4284 A) with four differing frequencies (1 KHz, 10 KHz, 100 KHz and 1 MHz) at a scope of temperature extending from 30 to 150 °C. The estimations of DC electrical conductivity were finished utilizing the customary two-test system for temperatures extending from 40 – 150 °C.

IV. EXPERIMENTATION AND ANALYSIS

A. Single Crystal XRD Analysis

Single crystal XRD information of $LA_xZnS_{(1-x)}$ crystals with various proportions are summarized in Table 1 along with correlation reason cross section parameters of unadulterated LA given in the table. It is observed that the developed $LA_xZnS_{(1-x)}$ crystals has a place with orthorhombic structure. Noteworthy change in the unit cell parameters affirms the nearness of $ZnSO_4$ in the LA crystal cross section. The grouping of $ZnSO_4$ in $LA_xZnS_{(1-x)}$ crystal builds, regardless of the cross section parameters (a, b and c).

Table 1:
Single crystal XRD data for $LA_xZnS_{(1-x)}$ crystals

Data	$LA_{0.8}ZnS_{0.2}$	$LA_{0.6}ZnS_{0.4}$	$LA_{0.4}ZnS_{0.6}$	$LA_{0.2}ZnS_{0.8}$
a (Å)	11.72	11.70	11.64	11.58
b (Å)	15.40	15.72	15.48	15.36
c (Å)	5.86	5.68	5.64	5.70
α°	90	90	90	90
β°	90	90	90	90
γ°	90	90	90	90
Crystal System	Orthorhombic	Orthorhombic	Orthorhombic	Orthorhombic

B. Powder X-ray Diffraction Analysis

The recorded Powder XRD examples of $LA_xZnS_{(1-x)}$ single precious stones are portrayed in Figure 3. The Bragg's diffraction crests were ordered for the orthorhombic framework with the space gather $P2_12_12_1$. The observed noticeable pinnacles affirm the crystalline property of the developed crystals. The PXRD designs got for $LA_xZnS_{(1-x)}$ precious stones (Figure 3) are all around coordinated with the unadulterated LA additionally some force are marginally moved, smothered and recently raised, this demonstrated the blended $ZnSO_4$ atoms considered in the present examination do not exasperate the crystal structure of LA cross sections [15]. The recently brought power crest up in powder XRD (Figure 3) affirmed the development of LAZnS single precious stones.

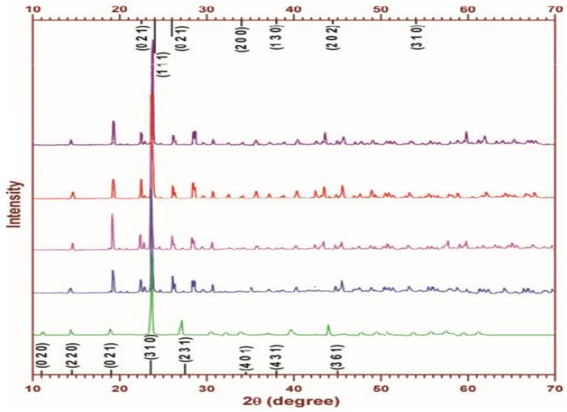

Figure 3:Indexed PXRD patterns of $LA_xZnS_{(1-x)}$ crystals

C. Fourier Transform Infra Red Analysis

The FT-IR spectral measurements were performed to analyze qualitatively the presence of various functional groups with vibrational frequencies and chemical bond connectivity in the developed admixture amino acids with cadmium sulphate. The FT-IR spectrum of LAZnS was recorded in the frequency region from 4000 to 450 cm^{-1} with Perkin Elmer FT-IR spectrometer using KBr pellets containing LAZnS powder and its various structural compositions were analyzed. The obtained FT-IR spectrum was shown in the Fig. 4.

The FT-IR transmission range of precious stones in the locale 4000-450 cm^1 is shown in figure 4. The assignments of the key vibrational modes due to $-COO^-$, NH_3^+, CH_2, CH bunches were made. The $-NH_2$ gathering of L-arginine is protonated by the - COOH gathering, offering ascend to NH_3^+ and $-COO^-$gatherings. The substantial covering in the prevalent vitality area 3040–3200 and 3400–3520 cm^{-1} is attributable to NH_3^+ symmetric, lopsided with extending vibrations, and the assimilation crest at 1625 cm^{-1} is doled out to NH_3^+ twisting savage mode. The carboxylic gathering was found to exist as the $-COO^-$, in the crystal. The solid top at 1360 and 1245 cm^{-1} additionally demonstrates the distinguishing proof of $-CH_2$ winding and $-CH_2$ swaying modes in the crystal grid. The more grounded CH_2 extending vibrations cover the CH extending vibrations beneath 3000 cm^{-1} [16-18].

It is outstanding that an ionized carboxylic gathering ($-COO^-$) has trademark wave numbers in the locales 1630–1520 cm^{-1} (solid hilter kilter extending), 1410 cm^{-1} (powerless symmetric extending) and 660 cm^{-1} (symmetric disfigurement). The crest at 1410 cm^{-1} is relegated to the symmetric extending mode. The area of retention groups from 3050 to around 2540 cm^{-1} was because of different blends of over tone groups; the solid assimilation at 1410 cm^{-1} relates to $-COO^-$ symmetric

 DOI : 10.18231/2454-9150.2018.1145

extend. The -COO^- twisting and shaking frequencies happen in the ordinary positions at 762, 622 and 536 cm^{-1}. Additionally the assimilation at 1340 and 1025 cm^{-1} has been due to -CH_3 symmetric twisting and shaking mode. The retention tops at 920 and 848 cm^{-1} have been allotted to C–N symmetric extending vibrations.

The zwitter ionic nature of the amino corrosive was obvious from NH_3^+ assimilation band and furthermore the -COO^- retention band at 1513 cm^{-1} (NH_3^+ symmetric bowing), 1422 cm^{-1} (-COO^- symmetric extending), 646 cm^{-1}(-COO^- bowing) and 418 cm^{-1} (-COO^-shaking) [17,18]. The C– CN extending vibration was affirmed by the nearness of crest at 918 cm^{-1}. Because of C-CH_3 twisting, a solid retention top was framed at 862 cm^{-1}. The bowing and shaking vibration of -COO^- were seen at 652 cm^{-1} and 418 cm^{-1} individually. The vibration at 1380 cm^{-1} was ascribed to C– C extending vibration. In general, a sulphate ion of $ZnSO_4$ ion has stretching vibrations at 1120, 990, 624 and 632 cm^{-1} [19]. Increasing absorption near 3500 cm^{-1} and developing new peaks at near1562 and 450 cm^{-1} in FT-IR spectrum, revealed that the presence of $ZnSO_4$ in grown crystal. The peak observed at 450 cm^{-1} has been assigned to the doubly degeneration of sulphate ion. The shoulder appeared at 1562 cm^{-1} and was due to bending vibrational modes of water molecule of zinc sulphate [20]. From the above discussion, the presence of all the fundamental functional groups of the sample has been confirmed qualitatively.

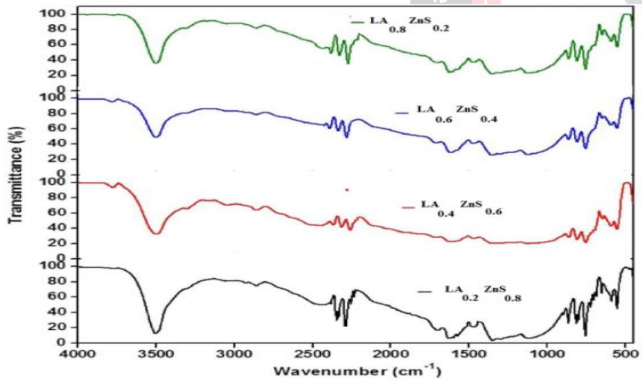

Figure 4: FT-IR spectra of $LA_xZnS_{(1-x)}$ crystals

D. Optical Absorption Spectrum Analysis

UV-Visible spectrum gives information about the structure of the molecules because the absorption of UV and Visible light involves promotion of the electron in the π orbital to the high energy π* orbital. The recorded spectra are shown in figure 5. In the present study, the optical behaviour was examined between 215 to 800 nm. The absence of absorption in the region between 250 and 800 nm in the UV-Vis spectrum showed that this crystal is good enough for the second harmonic generation of Nd-YAG laser of wavelength (1064 nm). It is a requirement or NLO materials having nonlinear optical applications [21]. Plot for deciding optical bandgap from UV-Visible spectrum of $LA_xZnS_{(1-x)}$ single precious stones are shown in figure 6. From figure 6, the UV cutoff wavelength of $LA_xZnS_{(1-x)}$ crystals diminishes with expanding grouping of $ZnSO_4$. It uncovers that the UV cutoff wavelength of $LA_xZnS_{(1-x)}$ crystals can be tuned by altering the convergence of $ZnSO_4$ in LA_xZnS. $LA_xZnS_{(1-x)}$, makes it appropriate for manufacturing optoelectronic gadgets according to our need. The ascertained bandgap vitality and UV cutoff wavelength of all the developed crystals were presented in Table 2.

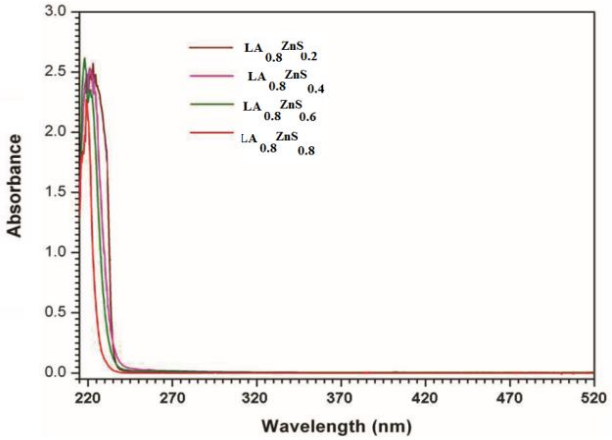

Figure 5: UV-Vis absorption spectrum of $LA_xZnS_{(1-x)}$ single crystals

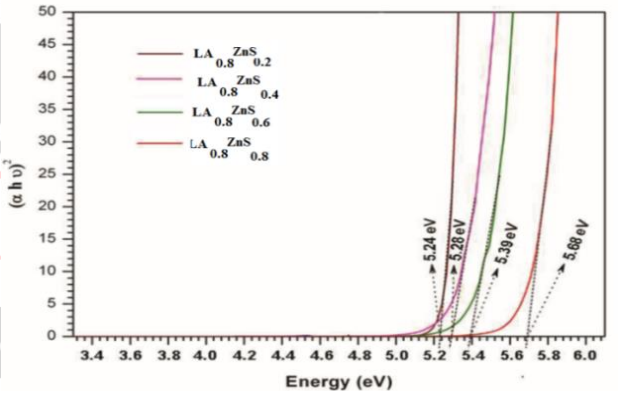

Figure 6 Plot of optical bandgap determination from UV-Vis absorption data of $LA_xZnS_{(1-x)}$ single crystals

The optical absorption spectrum of a good quality grown crystal was recorded using a Perkin Elmer Lamda 935 UV-vis-NIR spectrometer. The obtained absorption spectrum is shown in figure 5, where the lower cut off region is obtained at 246 nm. The UV spectra show the presence of a wide transparency window lying between 258 nm and 1000 nm. This study of UV spectra enables to understand the electronic structure of the optical band gap of the crystal. Also the knowledge about the absorption edge is needed to predict if the band structure is affected near the extreme ends of the band [22]. Hence, by analysing the absorption spectrum, it can be observed that the grown crystal is transparent in the entire visible region without any absorption peek. This property is

 DOI : 10.18231/2454-9150.2018.1145

actually preferred for any nonlinear optical crystal that supports second harmonic generation (SHG).

Table 2. Optical bandgap energy and cutoff wavelength of $LA_xZnS_{(1-x)}$ single crystals

Sample name	Optical bandgap energy (eV)	Cutoff wavelength (nm)
$LA_{0.8}ZnS_{0.2}$	5.20	252
$LA_{0.6}ZnS_{0.4}$	5.26	240
$LA_{0.4}ZnS_{0.6}$	5.38	236
$LA_{0.2}ZnS_{0.8}$	5.54	224

E. NLO Studies

The Nonlinear Optical (NLO) property of $LA_xZnS_{(1-x)}$ crystals were determined. The crystal was ground into uniform powder and after that pressed in a micro capillary of uniform bore and presented to a Q-exchanged Nd:YAG laser light emission 1064 nm with heart beat width of 8 ns and 10 Hz beat rate. The bar vitality of the Nd:YAG laser working at 1064 nm was set to 6.5 mJ/beat. The laser pillar was made to fall typically on the narrow tube and the yield from the example was monochromated to gather the force of 532 nm part. The age of second symphonious was affirmed by the outflow of green light. The yield control from $LA_xZnS_{(1-x)}$ precious stones were contrasted with that of KDP crystal and the outcomes are exhibited in Table 3.

Table 3: SHG and efficiency values of pure $LA_xZnS_{(1-x)}$ single crystals

Sample name	Input power mJ	Output power mV	SHG efficiency (compared with KDP)
$LA_{0.8}ZnS_{0.2}$	6.5	102.4	1.90
$LA_{0.6}ZnS_{0.4}$	6.5	118.0	2.24
$LA_{0.4}ZnS_{0.6}$	6.5	122.6	2.32
$LA_{0.2}ZnS_{0.8}$	6.5	128.8	2.46

For a laser input beat of 6.5 mJ, the second symphonious flag (532 nm) of 53 mV was acquired for KDP test. The SHG effectiveness of $LA_xZnS_{(1-x)}$ crystals are higher than the unadulterated LA crystal likewise SHG productivity increments with expanding $ZnSO_4$ fixation in $LA_xZnS_{(1-x)}$ crystals from 0.2 to 0.8 mole.

The most extreme SHG productivity got for $LA_{0.2}ZnS_{0.8}$ crystal is more noteworthy than 2.48 times from the KDP crystal. The great second symphonious age proficiency demonstrates that the diverse grouping of $ZnSO_4$ in $LA_xZnS_{(1-x)}$ crystals can be utilized for applications in nonlinear optical gadgets.

F. Microhardness Studies

Microhardness is important for good quality crystals along with good optical performance. Hardness of the crystal carries information about the strength, molecular binding, yield strength and elastic constants of the materials [23]. In the present study, micro hardness measurements were carried out on LA single crystals.

The mechanical property of LAZnS crystals was studied by Vickers hardness test. Three different loads namely 25, 50 and 100g were applied on the crystal. Different points on the crystal surface were marked to measure and the average value was taken as the Vickers hardness number for a given load. The formula used to compute Vicker's Hardness Number (hv) is:

$$hv = 1.8544\ Load/d\_length^2\ (kg/mm^2)$$

where $Load$ is the applied load in Kg and d_length is the average diagonal length of the indentation mark in mm.

The hardness values of grown crystals increase with increasing load. The reverse indentation size effect involves increase in hardness value with increasing load [24]. It is interesting to note that the hardness values of LAZnS are approximately doubled when compared to pure l-arginine [25]. Hardness values of different load are given in Table 4.

To evaluate the Vickers hardness, several indentations were made on the face of the crystal. The indentation related to diagonal length was computed using a micrometer eyepiece. Dependence of the microhardness on the load for LA crystal has been evaluated. Load of different magnitude (25 and 50 g) were applied on the LA crystal for the fixed interval of time. Hardness is found to decrease as the load increases. The measurement of Vickers microhardness values is as shown in Table 4. The load above 50g developed multiple cracks on the crystal surface due to the release of internal stresses generated locally by indentation. So, for the NLO applications the test is suggested below 50g of applied load. This implies that LA single crystal is a good engineering material for device fabrications.

Table 4. Hardness value of LAZnS.

Sl.No	Molecular composition of crystal	Applied load (gm)	Hardness Hv (kg/mm2)
1	$LA_{0.8}ZnS_{0.2}$	25	40
		50	44
		100	58
2	$LA_{0.6}ZnS_{0.4}$	25	40
		50	44
		100	58
3	$LA_{0.4}ZnS_{0.6}$	25	40
		50	44

 DOI : 10.18231/2454-9150.2018.1145

		100	58
4	$LA_{0.2}ZnS_{0.8}$	25	40
		50	44
		100	62

G. Dielectric Studies

The dielectric studies considered for all the developed crystals were carried out on the (1 2 0) plane. The varieties of dielectric steady, dielectric misfortune and AC electrical conductivity of $LA_xZnS_{(1-x)}$ precious stones at various temperatures running from 30 to 150 °C and diverse recurrence extending from 1 KHz to 1 MHz. are shown in Figures 7 – 9.

The electrical parameters, viz, dielectric steady, dielectric misfortune and AC electrical conductivity are increased with the increase in temperature for all the developed precious stones. The ε_r and tan δ esteems were diminished while the σ_{ac} esteem expanded with the expansion in recurrence of the AC connected for every one of the frameworks. It can be seen from Figures 7-9 that the dielectric misfortune at the low recurrence locale rises somewhat, as the temperature is increased from 30 to 150 °C for every one of the frameworks.

This can be clarified based on polarization and conduction forms, which are included when an electric field is connected to the developed crystals. The electronic trade of the quantity of particles in the crystal gives the nearby uprooting of electrons toward the connected field, which thus offers ascend to polarization, and when the recurrence increments to an ideal incentive there after the space charge cannot be managed and consent to the outside field and consequently the polarization diminishes [26].

The obtained dielectric consistent esteems for every one of the crystals at room temperature for 100 KHz recurrence were low. Additionally the dielectric misfortune diminishes with increment in recurrence at all temperatures. This sort of conduct is accomplished for every one of the precious stones considered in the present investigation. The enormous estimations of r at little frequencies might owe to the nearness of room charge, introduction, electronic and ionic polarizations. The low estimation of r at higher frequencies might be because of the loss of importance of this polarization slowly.

The bends demonstrate that the dielectric misfortune diminishes with increment of recurrence and increments with increment of temperature. The material with low dielectric steady has few dipoles/unit volumes. Therefore it has least misfortune when contrasted with the material with higher dielectric steady [27].

The normal for low dielectric misfortune with high recurrence for $LA_xZnS_{(1-x)}$ crystals recommends that the crystals have great optical quality with lesser deformities and this parameter is of indispensable significance for nonlinear optical materials in their applications. The little estimation of dielectric consistent at unrivaled recurrence is crucial for the utilization of these materials in the formation of photonic, electro-optic, NLO gadgets with various quantum well structures.

The AC conductivity of $LA_xZnS_{(1-x)}$ are high for higher frequencies at a given temperature and is shown in figures 7 through 9. From the figures, it can be seen that the conductivity increments with the increase of temperature and recurrence. It uncovers that the conductivity could be because of the lessening in the space charge polarization at higher frequencies.

It is found that the dielectric constant decreased in value with increasing frequency, at room temperature. The high value of dielectric constant at lower frequencies may be due to the presence of all the four polarization namely, space charge, orientation, ionic and electronic polarization and its low value at higher frequencies may be due to the loss of significance of these polarizations gradually [28]. Figure 8 shows the variation of dielectric loss with applied frequency and it was also observed that the dielectric loss was reduced at higher frequencies. The characteristic of low dielectric loss at higher frequency ranges shows that the LA crystal possesses good quality with lesser defect which is important for NLO applications [29].

The values of ε_r is high at low frequencies. This is owing to the presence of all the four polarizations namely, space charge, oriental, ionic and electric polarizations. The value of ε_r is low at high frequencies, which may be due to the loss of significance of these polarizations gradually. It is to be noted here that space charge polarization is dominant and electronic and ionic polarizations are not very much active in low frequency region [30]. The lower value of dielectric constant at higher frequencies makes it suitable for the enhancement of SHG coefficient [31]. The low value of dielectric loss at high frequency shows the high optical quality of the crystal with lesser defects, which is the desirable property for NLO applications.

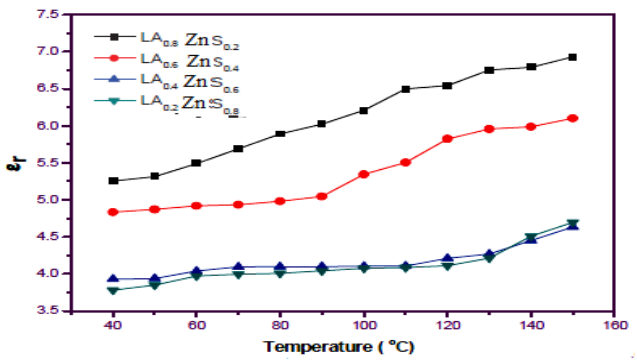

Figure 7: Dielectric constants measurement for 100 KHz frequency for $LA_xZnS_{(1-x)}$ single crystals

 DOI : 10.18231/2454-9150.2018.1145

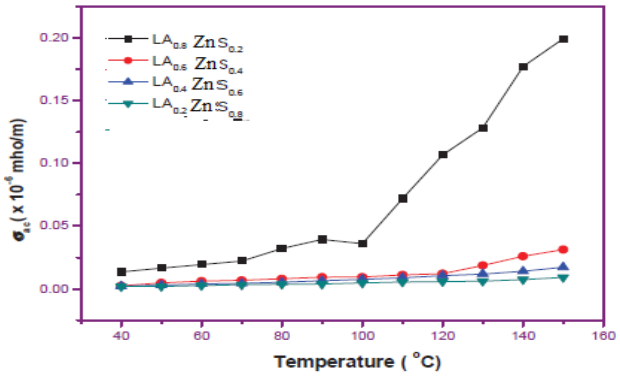

Figure 8: AC conductivity measurement for 100 Hz frequency for $LA_xZnS_{(1-x)}$ single crystals

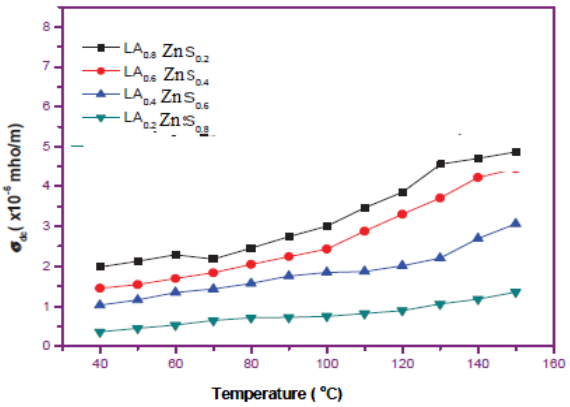

Figure 9: AC conductivity measurement for 100 KHz frequency for $LA_xZnS_{(1-x)}$ single crystals

H. Energy Dispersive X-ray Analysis

Energy dispersive X-ray analysis (EDAX) used in conjunction mode and all types of electron microscopes have become an important tool for characterizing the element present in the crystals. Fig.10 illustrates the EDAX spectrum of LAZnS crystals recorded on an accelerated voltage 15.0 kV, magnification ×1000, working distance 15.1 mm using JEOL company. The presence of $ZnSO_4$ in LAZnS is confirmed from the EDAX spectrum.

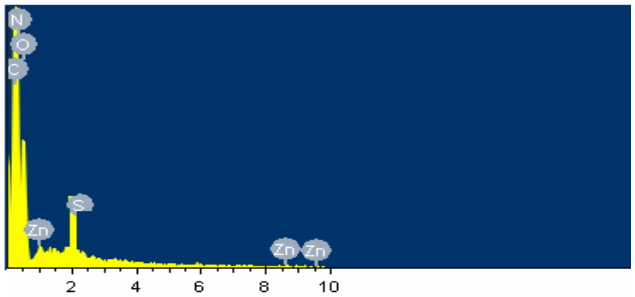

Figure 10 Energy dispersive X-ray analysis of LAZnS crystal

I. NMR Spectra

The ^1H and ^{13}C-NMR spectrum were recorded for the crystals dissolved in water (D_2O) using Bruker 300 MHz (ultrasheild)TM instrument at 23◦C (300 MHz for ^1H NMR and 75 MHz for ^{13}C NMR to confirm its molecular structure. The ^1H and ^{13}C NMR spectrum of LAZnS are shown in Figures 11 and 12.

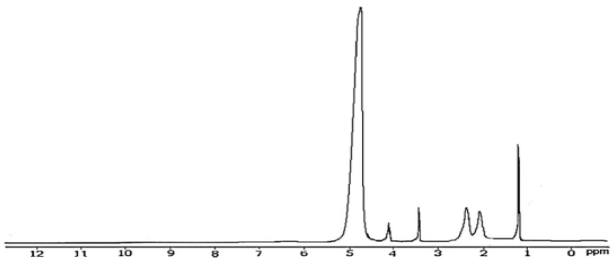

Figure 11 ^1H-NMR spectrum of LAZnS

The chemical shifts are represented in ppm and assigned by using web literature [10]. ^1H-NMR spectrum shows a doublet at δ = 1.15 ppm due to 3protons of CH_3 group. Another, doublet appears at δ = 3.40 ppm which corresponds to CH C group. The pentaplet at δ = 4.07 ppm corresponds to CH group. The singlet peak was observed at 4.68 δ ppm is due to presence of D_2O solvent.

From the comparison of pure l-arginine, ı values are shifted to downward for LAZnS crystal. This may be attributed to shielding effect of $ZnSO_4$ on l-arginine. The ^{13}C-NMR spectrum of LAZnS contains four signals. The carbonyl group resonates at δ = 172.80 ppm. The presence of carbon induced resonance peaks at δ = 60.36 ppm and δ = 65.84 ppm.

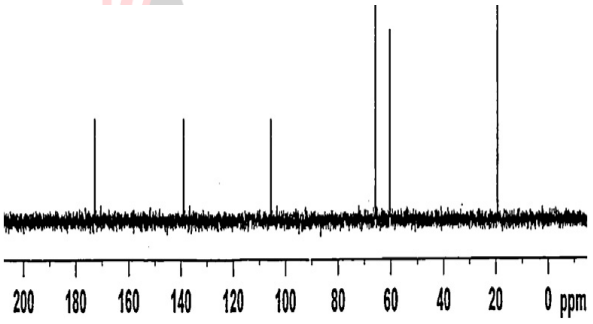

Figure 12 ^{13}C-NMR spectrum of LAZnS crystal

J. TGA Analysis

To study the thermal stability, thermo gravimetric analysis (TGA) and differential thermal analysis (DTA) were carried out for grown crystal. The thermo gravimetric analysis of Zn doped l-arginine crystals was done in nitrogen atmosphere in the temperature range 280C–800°C. The thermo grams of pure and Zn doped l-arginine are shown in Figure 13.

 DOI : 10.18231/2454-9150.2018.1145

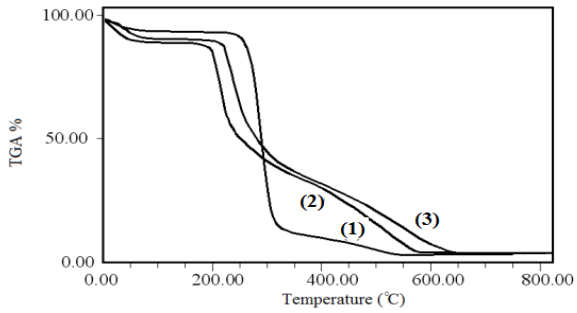

Figure 13.Thermogravimetric profile of LAZnS crystal in different compositions (i) $LA_{0.2}ZnS_{0.8}$, (ii) $LA_{0.6}ZnS_{0.4}$ and (iii) $LA_{0.4}ZnS_{0.6}$

The decomposition of l-arginine begins at 165°C. But for Zn doped l-arginine crystals, the decomposition starts at 205°C. The compound starts to lose single molecules of water of crystallization around 100°C. The weight loss in this temperature range is consistent with the weight of single molecules of water present in the crystal. The increment in the decomposition temperature is evident for the doped crystals, suggesting that the incorporation of zinc enhanced thermal stability. From the thermal studies, it is observed that melting point of grown crystal has been increased when compared to that of pure l-arginine (205◦C [32]) and may be due to the incorporation of $ZnSO_4$ which strengthens bonds within the crystal.

K. Second harmonic generation

The first and the most widely used technique for confirming the second harmonic generation (SHG) from prospective second order NLO material is the Kurtz and Perry powder technique [33]. The SHG behaviour was confirmed by the output of intense green light emission from the crystal. The measured output of LTMS was 11 mV. For the same input, KDP crystal emitted the green light with the output power of 11 mV. The SHG efficiency of LAZnS is higher than that of some of amino acid family materials [34–36] and is shown in Table 5.

Table 5 SHG efficiency of LAZnS and amino acid family.

Sl.No	Composition of crystal	SHG efficiency with respect to KDP
1	$LA_{0.8}ZnS_{0.2}$	1.00
2	$LA_{0.6}ZnS_{0.4}$	1.60
3	$LA_{0.4}ZnS_{0.6}$	2.40
4	$LA_{0.2}ZnS_{0.8}$	3.20
5	KDP	1.00

L. Birefringence Study

Birefringence analysis is a precise technique to find the optical perfection and optical homogeneity in crystals. The birefringence values have been calculated by finding absolute fringe orders using the relation:

$$\Delta n = k\lambda / t$$

Where, λ is wave length, t is the thickness of the crystal and k is the order of fringe.

Figure 14 shows the variation of birefringence with the wavelength and it shows that the birefringence values lie in between 0.028 to 0.084 in the wavelength ranging from 241 nm to 800 nm. The slight variation in birefringence over a wide range of wavelength indicates that the crystal is suitable material for second and third harmonic generation device fabrication. The obtained birefringence values were found to be positive which increased with increasing wavelength. A minimum dispersion in birefringence can be the key factor in frequency conversion process such as second and third harmonic generations.

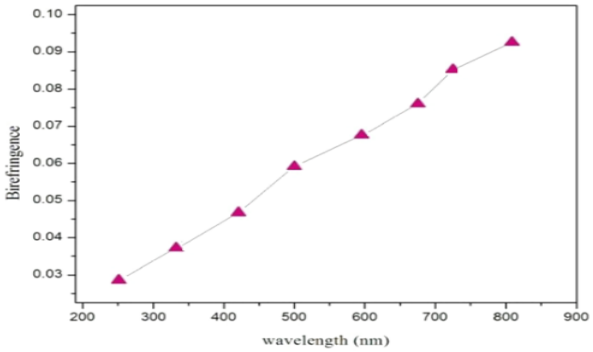

Figure 14. Birefringence spectrum of LAZnS crystal

V. CONCLUSION

Optically transparent, single crystals of Good quality, single crystals of $ZnSO_4$ doped L-arginine (LA) were grown successfully by slow evaporation technique. The powder XRD studies confirm the structure of the doped crystals to be similar to that of the pure one. The presence of the dopant has marginally altered the lattice parameters without affecting the basic structure of crystal. The lower UV cut-off wavelength of the examples retained at underneath 245 nm is an attractive parameter for NLO crystals. The NLO property was affirmed utilizing Nd : YAG laser of wavelength 1064 nm and the productivity of unadulterated LA and $LA_xZnS_{(1-x)}$ were assessed to be 2.48 times higher than that of KDP. Curiously, $LA_{0.2}ZnS_{0.8}$ is better than unadulterated LA and different groupings of $LA_xZnS_{(1-x)}$. The microhardness powder shows that every one of the crystals have a place with the class of hard materials.

The thermal stability is found to be better for the obtained crystal. Also the UV absorption edge has moved towards the blue region, thereby increasing the transparency region from the IR to the middle of UV. The decrease in the dielectric constant of the Zinc sulphate doped LA compared to pure LA can be attributed to better crystal perfection in the doped sample. The second harmonic

 DOI : 10.18231/2454-9150.2018.1145

generation efficiency for the doped LA sample has increased to a great extent making the doped crystal suitable for NLO applications. The nonlinear absorption coefficient of the doped crystal is also found to be increased so that it can be used as an optical limiter as well.

Good mechanical properties, excellent optical quality, moderate thermal stability and increased SHG efficiency, make the $ZnSO_4$ doped LA crystals a strong candidate for NLO device applications. As the characteristics of the crystal were found to be high, it finds potential applications in the area of optoelectronics. In the UV spectrum, the resultant crystal is found to be transparent and it could be a useful candidate for optoelectronic applications in visible and infrared region.

REFERENCES

[1] H.V. Alexandru, J. Cryst. Growth 169 (1996) 347.

[2] Y. Asakuma, Q. Li, H.M. Ang, M. Tade, K. Maeda, K. Fukui, Appl. Surf. Sci. 254(2008) 4524.

[3] X. X. Ren, D. D. Xu, D. D. Xue, J. Cryst. Growth 310 (2008) 2005.

[4] Z. Li, X. Huang, D. Wu, K. Xiong, J. Cryst. Growth 222 (2001) 524.

[5] A.S. Haja Hammeed, G. Ravi, R. Ilangovan, A. Nixon Azariah, P. Ramasamy, J.Cryst. Growth 237 (2002) 890.

[6] V. Kannan, R. Bairava Ganesh, P. Ramasamy, Cryst. Growth Des. 6 (8) (2006)1876.

[7] P.M. Ushasree, R. Jayavel, P. Ramasamy, Mater. Chem. Phys. 61 (1999) 270.

[8] D.V. Isakov, F.P. Ferreira, J. Barbosa, J.L. Ribeiro, E. de Matos Gomes, M.S. Belsley,Appl. Phys. Lett. 90 (2007) 073505.

[9] D. Yuan, Z. Zhong, M. Liu, D. Xu, Q. Fang, Y. Bing, S. Sun, M. Jiang, J. Cryst. Growth186 (1998) 240.

[10] G. Anandha babu, G. Bhagavannarayana, P. Ramasamy, J. Cryst. Growth 310(2008) 2820–2826.

[11] R. Bairava Ganesh, V. Kannan, K. Meera, N.P. Rajesh, P. Ramasamy, J. Cryst.Growth 282 (2005) 429–433.

[12] P. Rajesh, P. Ramasamy, C.K. Mahadevan, J. Cryst. Growth 311 (2009)1156–1160.

[13] Martin Britto Dhas S.A., Bhagavannarayana G. and Natarajan S., The open crystalo. J., 1, 42-45 (2008).

[14] Karunanithi U., Arulmozhi S. and Madhavan J., J. Appl. Phys., 1(2), 14-18 (2012)

[15]Mohan Kumara R., Rajan Babub D., Jayaramanc D., Jayaveld R. and Kitamura K., J. Cryst. Growth, 275, 1935-1939 (2005)

[16] Arun K.J. and Jayalekshmi S., J. Minrl. Mater. Char. & Engr., 8(8), 635-646 (2009)

[17] Praveen Kumar P., Manivannan V., Sagayaraj P. and Madhavan J., Bull. Mater. Sci., 32(4), 431-435 (2009).

[18] P. Pramasivam, M. Arivazhagan, C. Ramachandraraja, Indian Journal of Pure and Applied Physics, 49, 394 (2011).

[19] M. Iyanar, J. Thomas Joseph Prakash, C. Muthamizhchelvan, S. Ponnusamy, Journal of Physical Sciences, 13, 235 (2009).

[20] S. Ruby, Alfred Cecil Raj, International Journal of Scientific and Research Publications, 3 (3), 1, (March 2013).

[21] N. Vijayan, R. Ramesh Babu, Journal of Crystal Growth, 236, 407 (2002).

[22] T. J. Bruno, P.D.N. Srorws, Hand book of Basic Tables for Chemical Analysis -Second Edition, CRC Press.

[23] Tiverios C. Vaimakis, Thermogravimetry (TG) or Thermogravimetric Analysis (TGA) Chemistry Department, University of Ioannina, Ioannina, Greece.

[24] A. Ruby, S. Alfred Cecil Raj, International Journal of ChemTech Research 5 (1), 482, (2013). [25] J. Thomas Joseph Prakash, L. Ruby Nirmala, International Journal of Computer Applications, 6 (7), 975, (2010).

[26] P. Malliga, Journal of Chemical and Pharmaceutical Research, 6 (12), 359 (2014).

[27] A. Suvitha, P. Murugakoothan, Spectrochimica Acta Part A, 86, 266, (2012).

[28] M. R. Jagadeesh, H. M. Suresh Kumar, R. Ananda Kumari, Archives of Applied Science Research, 6 (4), 88–197, (2014).

[29] J. Kishore Kumar, G. Anand, S. Gunasekaran, P. Hemalatha, S. Kumaresan, Elixir Crystal Growth, 61, 17110–17114 (2013).

[30] R. Rajasekaran, R. Mohan Kumar, R. Jayavel, P. Ramasamy, Journal of Crystal Growth 252, 317–327, (2003).

[31] Redrothu Hanumantharao, S. Kalainathan, Spectrochimica, Acta Part A 86, 80–84, (2012).

[32] Iyanar, C. Muthamizhchelvan, S. Ponnusamy, J. Thomas Joseph Prakash, Recent Research in Science and Technology, 2 (1), 97 (2010).

[33] S. Suresh, R. Vasanthakumari, Rasayan Journal of Chemistry, 2 (2), 446 (2009).

[34] T. Thaila, S. Kumararamanan, Archives of Applied Science Research, l4 (3), 1494, (2012). [35] R.Muralidharan, R. Mohankumer, P.M.Ushasree, R. Jayavel, P.Ramasamy, Journal of Crystal Growth, 234, 545 (2002).

[36] J. Baran, M. Drozd, A. Pietrazico, M. Trzebiatowska, H. Ratajczak, Journal of Polish chemistry, 77, 1561 (2003).

 DOI : 10.18231/2454-9150.2018.1145